Available online at www.sciencedirect.com
SCIENCE DIRECT
Phytochemistry 67 (2006) 5–12
PHYTOCHEMISTRY
www.elsevier.com/locate/phytochem

Transition state analysis of adenosine nucleosidase from yellow lupin (*Lupinus luteus*)

Carl Bates, Zachariah Kendrick, Nancy McDonald, Paul C. Kline *

Department of Chemistry, Middle Tennessee State University (MTSU), Box 68, Murfreesboro, TN 37132, United States

Received 2 May 2005; received in revised form 24 August 2005
Available online 21 November 2005

Abstract

The transition state of adenosine nucleosidase (EC 3.2.2.7) isolated from yellow lupin (*Lupinus luteus*) was determined based upon a series of heavy atom kinetic isotope effects. Adenosine labeled with ^{13}C, ^{2}H, and ^{15}N was analyzed by liquid chromatography/electrospray mass spectrometry to determine kinetic isotope effects. Values of 1.024 ± 0.004, 1.121 ± 0.005, 1.093 ± 0.004, 0.993 ± 0.006, and 1.028 ± 0.005 were found for [1′-^{13}C], [1′-^{2}H], [2′-^{2}H], [5′-^{2}H], and [9-^{15}N] adenosine, respectively. Using a bond order bond energy vibrational analysis, a transition state consisting of a significantly broken C–N bond, formation of an oxocarbenium ion in the ribose ring, a conformation of C3-*exo* for the ribose ring, and protonation of the heterocyclic base was proposed. This transition state was found to be very similar to the transition state for nucleoside hydrolase, another purine metabolizing enzyme, isolated from *Crithidia fasciculata*.

Keywords: Yellow lupin; *Lupinus luteus*; Kinetic isotope effects; Transition state; Adenosine nucleosidase

1. Introduction

Adenosine nucleosidase (EC 3.2.2.7) is an enzyme of the purine salvage pathway and has been implicated in a number of physiological roles including controlling the level of cytokinins, synthesis of caffeine, and synthesis of *S*-adenosyl-L-methionine (Chen and Kristopeit, 1981; Koshiishi et al., 2001; Edwards, 1996). It is a hydrolytic enzyme that catalyzes the irreversible hydrolysis of various nucleosides to ribose and the corresponding base.

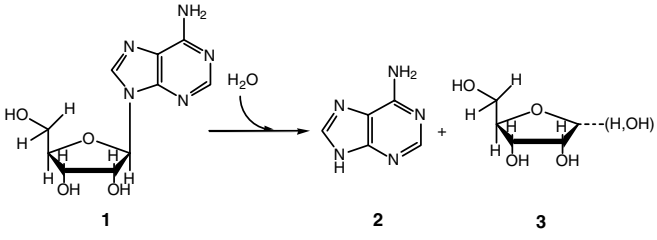

1 2 3

Adenosine nucleosidase activity has been detected in a number of plants with the enzyme level varying widely from one species to another (Leszczynska et al., 1984). The enzyme has been isolated from a number of plant sources including Jerusalem artichoke shoots, tomato roots and leaves, spinach beet leaves, barley leaves, tea leaves, wheat germ, coffee leaves, malted barley, and yellow lupin (Le Floc'h and Lafleuriel, 1981; Burch and Stuchbury, 1986; Poulton and Butt, 1976; Guranowski and Schneider, 1977; Imagawa et al., 1979; Chen and Kristopeit, 1981; Campos et al., 2005; Lee and Pyler, 1986; Abusamhadneh et al., 2000).

Abbreviations: LC/MS, liquid chromatography/mass spectrometry; KIE, kinetic isotope effect; HMDS, hexamethyldisilazine; Tris, tris(hydroxymethyl)aminomethane; SIM, selective ion monitoring; BEBOVIB, bond energy bond order vibrational analysis; RNA, ribonucleic acid; NAD^{+}, nicotinamide dinucleotide; AMP, adenosine monophosphate; IU-NH, inosine–uridine nucleoside hydrolase; IAG-NH, inosine–adenosine–guanosine nucleoside hydrolase.

* Corresponding author. Tel.: +1 615 898 5466; fax: +1 615 898 5182.
E-mail address: pkline@mtsu.edu (P.C. Kline).

0031-9422/$ - see front matter © 2005 Elsevier Ltd. All rights reserved.
doi:10.1016/j.phytochem.2005.10.006

Adenosine nucleosidase from yellow lupin is a dimer with a molecular weight of 72,000 (Abusamhadneh et al., 2000). The enzyme displays broad substrate specificity exhibiting activity with a variety of purine nucleosides including adenosine **1**, guanosine, inosine, 2-deoxyadenosine, and 5-deoxyadenosine. In contrast to other plant purine hydrolases for which the pH optimum has been reported to range from 4.0 to 6.5, the pH optimum for the reaction catalyzed by yellow lupin adenosine nucleosidase is 7.5 (Burch and Stuchbury, 1986; Imagawa et al., 1979; Abusamhadneh et al., 2000).

Purine hydrolases, such as adenosine nucleosidase, have been isolated from a number of other sources in addition to plants including protozoan parasites, yeast, and *Escherichia coli* (Parkin et al., 1991a; Shi et al., 1999; Versées et al., 2001; Pelle et al., 1998; Parkin, 1996; Miller et al., 1984; Kurtz et al., 2002; Petersen and Moller, 2001). The presence of these purine salvage enzymes has not been detected in mammals, which rely on a different set of enzymes to supply their nucleosides (Gopaul et al., 1996).

Nucleoside hydrolase (EC 3.2.2.1) isolated from *Crithidia fasciculata*, an insect parasite, is the most extensively studied of these hydrolytic enzymes. The enzyme has been purified to homogeneity and the substrate specificity, pH profile, and kinetic mechanism determined (Parkin et al., 1991a). In addition the catalytically important amino acids have been determined by site-directed mutagenesis and X-ray crystallography (Gopaul et al., 1996; Degano et al., 1996). Finally, the transition state has been determined using heavy atom kinetic isotope effects, and a new class of C-nucleoside analogs have been designed based upon that transition state (Horenstein et al., 1991, 1993).

The transition state structure provides insight into the multiple interactions that take place between the substrate and enzyme in an enzyme-catalyzed reaction. In addition, knowledge of the transition state allows the possibility of the design of highly specific inhibitors (Schramm et al., 1994). These inhibitors have the potential for a number of uses including controlling the growth of a particular plant or the analysis of a metabolic pathway. This study presents the transition state of adenosine nucleosidase, a nucleoside hydrolase isolated from yellow lupin, and compares it to the transition state of the *C. fasciculata* enzyme.

2. Results and discussion

2.1. Kinetic isotope effects

A family of heavy-atom kinetic isotope effects (KIE) for adenosine nucleosidase from yellow lupin were determined using [9-^{15}N], [1′-^{13}C], [1′-^{2}H], [2′-^{2}H], and [5′-^{2}H]adenosine **1** as substrates. These sites have been shown to be important in the determination of the transition state for other purine hydrolases. Substantial kinetic isotope effects were observed for [9-^{15}N], [1′-^{13}C], [1′-^{2}H] and [2′-^{2}H]adenosine **1**, while no significant kinetic isotope effect was observed for [5′-^{2}H]adenosine. These KIEs were used to determine the transition state of the enzyme-catalyzed purine hydrolysis reaction carried out by adenosine nucleosidase. The isotope effects determined for this reaction are listed in Table 1. A transition state based upon these KIEs is proposed (Fig. 1B). The proposed transition state gave the best agreement between the observed KIEs and a set of predicted KIEs using a bond-order bond-energy analysis. A cutoff model was used in calculating the transition state using BEBOVIB. The atoms used in this model were those in the ribosyl ring and imidazole ring but eliminated the hydroxyl hydrogens along with the 3-hydroxyl group. This model is similar to that used to calculate the transition state for other purine hydrolase and is based on the criteria of Stern and Wolfsberg (1966).

Table 1
Kinetic isotope effects for adenosine nucleosidase from yellow lupin

Substrate	Isotope and type of effect[a]	Kinetic isotope effect[b]
[1′-^{13}C]adenosine **1**	Primary	1.024 ± 0.004
[1′-^{2}H]adenosine **1**	α-Secondary	1.121 ± 0.005
[2′-^{2}H]adenosine **1**	β-Secondary	1.093 ± 0.004
[5′-^{2}H]adenosine **1**	δ-Secondary	0.993 ± 0.006
[9-^{2}N]adenosine **1**	Primary	1.028 ± 0.005

[a] A primary isotope effect has the label in the bond being broken. A secondary isotope effect indicates the label is one (α), two (β), or four (δ) bonds away from the breaking bond.

[b] Each isotope effect was the minimum of 12 individual determinations. The kinetic isotope effects were calculated using Eq. 2 in Section 3.

The [1′-^{13}C]adenosine **1** kinetic isotope effect was 1.024 ± 0.004. This primary KIE, along with the [9-^{15}N] KIE, reports on the extent to which the C1–N9 glycosidic bond is broken in purine nucleosides. Based upon the BEBOVIB calculations, the bond order between C1–N9 required to match this isotope effect is reduced from 1.09 to 0.25. The bond orders reported in this paper are calculated using Pauling's equation relating bond order to bond length

$$\mathbf{n}_{ij} = \mathbf{e}^{(r_1 - r_{ij})/0.3}, \quad (1)$$

where $\mathbf{n}_{ij}$ is the Pauling bond order between the two atoms, r_1 is the standard single bond length in Å, and r_{ij} is the length in Å between the two atoms. Using Pauling's bond order equation this corresponds to an increase in bond length from 1.47 to 1.92 Å for the C1–N9 bond.

The observed [1′-^{13}C]KIE is consistent with the formation of an oxocarbenium ion in the transition state similar to that seen for nucleoside hydrolase from *C. fasciculata* (IU-NH) (Horenstein et al., 1991). The [1′-^{14}C]KIE for IU-NH is 1.044 ± 0.004. To directly compare the two isotope effects requires the use of the Swain–Schaad relationship of $^{14}C = {}^{13}CKIE^{1.9}$ (Melander and Saunders, 1980; Swain et al., 1958). Based on this relationship the [1′-^{13}C]KIE for yellow lupin adenosine nucleosidase is equivalent to the [1′-^{14}C]KIE observed for IU-NH.

The [2′-^{2}H]adenosine **1** KIE is 1.093 ± 0.004. This β secondary effect is indicative of two important aspects of the enzyme-catalyzed reaction. The first is the nature of the

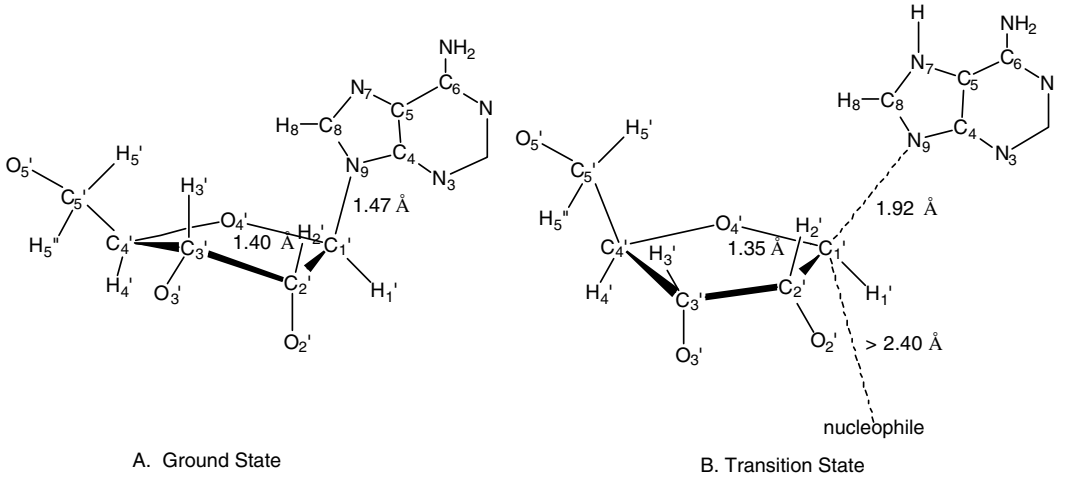

Fig. 1. Ground and transition states for adenosine nucleosidase (the hydroxyl hydrogens are omitted for clarity). (A) The ground state of adenosine was based upon the crystal structure reported by Lai and Marsh followed by energy minimization using Spartan 5 and Gaussian 98W. The bond lengths (in Å) are shown for the most important points. The conformation of the ribose ring is C3-*endo*. (B) The transition state of adenosine **1** gave the best match between the observed and BEBOVIB calculated kinetic isotope effects. The main features of the transition state are a substantially, but not completely broken C1–N9 bond, very low bond order to the attacking nucleophile, a change in ribose conformation from C3-*endo* to C3-*exo*, a decrease in C1–O4 bond length as the oxocarbenium ion forms, and protonation of the heterocyclic base at N7.

transition state. This KIE is consistent with the formation of an oxocarbenium ion predicted by the [1′-^{13}C]KIE. The [2′-^{2}H]KIE also reports on the ring conformation. With the increasing double bond nature of the C1–O4 bond, the ribose ring may assume two possible conformations: C3-*exo* or C3-*endo* (Horenstein et al., 1991; Berti and Tanake, 2002). In the C3-*exo* conformation the dihedral angle between C2–H2 and the empty p orbital is approximately 10° allowing hyperconjugation. in the C3-*endo* conformation the dihedral angle is much larger, reducing hyperconjugation. Matching the large β secondary KIE reported for this enzyme required that the sugar assume a conformation in the transition state in which hyperconjugation is possible, thus requiring a shift from the C3-*endo* conformation in the ground state to C3-*exo* conformation. The large [2′-^{2}H]KIE seen for this enzyme is similar to the [2′-^{2}H]KIEs reported for other purine hydrolases including IU-NH. As noted by Berti all of the reported 2 KIEs for this class of enzyme (with one exception) are greater than 1.1 for tritium KIEs and 1.065 for deuterium KIEs (Berti and Tanake, 2002). The single exception noted by Berti and Tanaka was for the RNA hydrolysis catalyzed by ricin A-chain toxin in which the [2′-^{2}H]KIE was reported to be 1.012 ± 0.005 (Chen et al., 2000). This small KIE was interpreted as indicating the ribose ring in the transition state had assumed a C3-*endo* conformation.

The [1′-^{2}H]adenosine **1** KIE for adenosine nucleosidase is 1.121 ± 0.005. The large α secondary [1′-^{2}H]KIE has also been interpreted to be consistent with the formation of an oxocarbenium ion in which the C–N bond is significantly broken, but there is little bond order to the attacking nucleophile (Poirier et al., 1994; Koerner et al., 2000; Matsson and Westaway, 1998). The observed KIE for this enzyme fits the observed KIEs for other purine hydrolases where the ^{2}H-KIE has been observed to range from 1.08 to 1.17 (Berti and Tanake, 2002). The large effect is due to the increased freedom around C1 as it undergoes rehybridization in the formation of the oxocarbenium ion (Poirier et al., 1994; Koerner et al., 2000; Matsson and Westaway, 1998).

Of all the KIEs measured in this study, the [1′-^{2}H] KIE is the most difficult to interpret quantitatively. This KIE is extremely sensitive to small changes in the C1–H1 bond order. As pointed out by Berti, because of the closeness of the oxocarbenium ion to H1 there are likely to be non-covalent interactions involved in the stabilization of the transition state that would affect the magnitude of [1′-^{2}H]KIE.

With a [5′-^{2}H]adenosine **1** KIE of 0.993 ± 0.005 for yellow lupin adenosine nucleosidase, there is no significant KIE at this remote location. This is in contrast to the results for other purine hydrolases such as IU-NH from *C. fasciculata* (EC 3.2.2.1), NAD^{+} hydrolysis by diphtheria toxin A-chain, and AMP nucleosidase from *Azotobacter vinelandii* (EC 3.2.2.4), all of which exhibited significant KIEs at the 5 position (Horenstein et al., 1991; Berti et al., 1997; Parkin et al., 1991b). These results have been interpreted to indicate that the hydroxyl group in the transition state is placed in such a position as to stabilize the positive charge on the oxocarbenium ion. Support for this interpretation was observed in the X-ray structure of IU-NH co-crystallized with *p*-aminophenyliminoribitol in which the hydroxymethyl group is positioned above the positive charge on the 5-membered ring. In contrast the 5 KIE for adenosine nucleosidase was similar to the [5′-^{3}H]KIE for the acid-catalyzed hydrolysis of AMP of 1.006 ± 0.005 and the solvolysis of NAD^{+} of 1.000 ± 0.003 (Mentch et al., 1987; Berti and Schramm, 1997). The lack of a KIE at the 5 position indicates that in the reaction catalyzed by adenosine nucleosidase the

hydroxymethyl group plays no role. This interpretation is also consistent with the substrate specificity of the enzyme. 5-Deoxyadenosine is a better substrate for the enzyme than is adenosine indicating the hydroxymethyl group does not take part in stabilizing the transition state (Abusamhadneh et al., 2000).

The [9-^{15}N]adenosine **1** KIE is substantial at 1.028 ± 0.005. This isotope effect along with the [1′-^{13}C] isotope effect reflects the extent to which the C1–N9 glycosidic bond is broken in the transition state. The magnitude of this KIE indicates the C1–N9 bond is substantially but not completely broken. A completely broken C1–N9 bond would yield a [9-^{15}N]adenosine **1** KIE of 1.04. To match the observed isotope effect the C1–N9 bond order was reduced to approximately 0.25 which is similar to the result predicted by the [1′-^{13}C]adenosine **1** KIE. The extent to which the C1–N9 bond is broken in the transition state of adenosine nucleosidase is similar to the 0.225 ± 0.095 bond order reported for IU-NH.

This kinetic isotope effect also reports on electronic rearrangements that may take place in the purine base in the transition state. Matching the observed [9-^{15}N]adenosine **1** KIE required the activation of the purine base by protonation of N7. Protonation turns the relatively poor leaving group of the heterocyclic base into a good leaving group. In addition protonation aids in the breaking of the C1–N9 bond by causing a decrease in the electron density within the purine ring. Protonation of N7 is also consistent with the mechanism proposed for the acid-catalyzed hydrolysis of purine nucleosides (Garrett and Mehta, 1972). Further evidence of the requirement for N7 protonation may be found in the substrate specificity of the enzyme (Abusamhadneh et al., 2000). Tubercidin (7-deazaadenosine), a nucleoside analog in which N7 has been replaced with a carbon, is not a substrate for this enzyme.

2.2. Transition state

Combining the results from the family of kinetic isotope effects results in a transition state whose main features are: (a) a highly dissociative transition state in which the C–N glycosidic bond is extensively broken while there is yet little bond formation between C1 and the attacking nucleophile; (b) formation of an oxocarbenium ion between C1 and 04; (c) a change in the ribose ring conformation from C3-*endo* in the ground state to C3-*exo* in the transition state; and (d) protonation of N7 of the heterocyclic base. This transition state is similar to the reaction catalyzed by other purine hydrolases.

In IUPAC nomenclature nucleophilic reactions can be described as either A_ND_N or $A_N + D_N$ where A_N is a nucleophilic addition and D_N is a nucleophilic displacement (Guthrie and Jencks, 1989). A_ND_N reactions are bimolecular S_N2 reactions while the $A_N + D_N$ reactions are unimolecular S_N1-type reactions. The S_N1 reaction can be further classified as either $A_N + D_N$ or $A_N * D_N$ in which $A_N + D_N$ describes a reaction in which the cationic intermediate is stable enough for the leaving group to diffuse away, or $A_N * D_N$ in which the intermediate is less stable and there is not enough time for the leaving group to diffuse away from the reaction site.

Several lines of evidence point to this reaction being an A_ND_N reaction. The primary [1′-^{13}C]adenosine **1** KIE has been used to distinguish the class of mechanism. A_ND_N reactions yield significant [1′-^{13}C]adenosine **1** KIEs of 1.03–1.08 while the isotope effects are significantly smaller, 1.00–1.01, for the $A_N * D_N$ mechanism (Berti and Tanake, 2002). The observed [1′-^{13}C]adenosine **1** KIE for adenosine nucleosidase is 1.024 ± 0.004 consistent with an A_ND_N mechanism.

Results from the BEBOVIB modeling also indicate the reaction is bimolecular consistent with an A_ND_N mechanism. While there is extremely low bond order between the attacking nucleophile and the substrate, it was necessary to include an interaction between the substrate and the nucleophile to match the observed KIEs. Therefore, while the reaction is not synchronized, it is still an A_ND_N reaction, although a highly dissociative one. This mechanism is the same as found for a number of N-riboside hydrolases including *E. coli* nucleoside hydrolase, *C. fasciculata* nucleoside hydrolase, AMP nucleosidase from *A. vinelandii*, and for the hydrolysis of NAD^+ by diphtheria toxin among others (Horenstein et al., 1991; Berti et al., 1997; Mentch et al., 1987).

The majority of protozoan nucleoside hydrolases belong to one of three groups based upon substrate specificity (Versées and Steyeart, 2003). One group consists of the base-specific *E. coli* IU-NH, while the second group consists of purine-specific nucleoside hydrolases (Estupiñán and Schramm, 1994), and the third group consists of 6-oxopurine specific nucleoside hydrolases. Of these three groups, adenosine nucleosidase from yellow lupin fits most closely with the second group based on base specificity. Other examples of this group include the nucleoside hydrolases from *Trypanosoma vivax* and *Trypanosoma brucei brucei* (Versées et al., 2001; Parkin, 1996). However, further examination indicates significant differences in substrate specificity of these nucleoside hydrolases and yellow lupin adenosine nucleosidase. The nucleoside hydrolases characterized to date use ribonucleosides as substrates, while the 2, 3, or 5 deoxyribonucleosides are not substrates or are extremely poor substrates. For example in the IAG-NH (EC 3.2.2.1) from *T. vivax* the k_{cat}/K_m is reduced by 1700, 2.3×10^5, and 7100 for 2-deoxyadenosine, 3-deoxyadenosine, and 5-deoxyadenosine, respectively, compared to the k_{cat}/K_m for adenosine. for IAG-NH from *T. vivax* all three hydroxy groups take part in the reaction (Versées et al., 2002). In contrast adenosine nucleosidase uses both 2-deoxyadenosine and 5-deoxyadenosine as substrates at a level comparable to that of adenosine **1**. In fact, 5-deoxyadenosine was the best substrate tested. The nucleoside hydrolases characterized to date are metalloproteins with a unique topology (Murzin et al., 1995; Orengo et al., 1997). In IU-NH, a calcium ion in the active site is believed to coordinate to the 2

and 5 hydroxyl group of the substrate and to the attacking nucleophile (Degano et al., 1998). IU-NH has multiple contacts between the enzyme and the ring deriving most of its catalytic efficiency by distortion of the ribosyl ring (Degano et al., 1996). A number of carboxylate residues hydrogen bond to the ribose ring causing a distortion, which allows the oxocarbenium ion to form. The question of how yellow lupin adenosine nucleosidase forces the ribose ring into the transition state conformation in the absence of the 2-OH group remains to be answered.

Mazzella et al. (1996) have identified three ways in which the purine hydrolases reach the transition state. They are activation of the leaving group by protonation of the purine base, stabilization of the oxocarbenium ion by interactions between the enzyme and ribose of the substrate, and ionization of the 2-hydroxyl group to stabilize the oxocarbenium ion. Enzymes may rely on one of these effects or use some combination of the above. For example of the 17.7 kcal/mol decrease in the energy of activation for the reaction catalyzed by IU-NH, the relative contributions of protonation/activation of the leaving group and stabilization of the oxocarbenium ion are 4.6 and 13.1 kcal/mol, respectively (Gopaul et al., 1996).

It seems likely that protonation of the leaving group provides the major contribution to the decrease in the energy of activation for adenosine nucleosidase. This is based upon substrate specificity since 2-deoxyadenosine is a substrate for adenosine nucleosidase, but it is not for IU-NH.

Based on a family of kinetic isotope effects a transition state was proposed for the hydrolysis of purine nucleosides by adenosine nucleosidase. The main features of the transition state are: (a) a highly dissociative transition state in which the C–N glycosidic bond is extensively broken while there is yet little bond formation between C1 and the attacking nucleophile; (b) formation of an oxocarbenium ion between C1 and O4; (c) a change in the ribose ring conformation from C3-*endo* in the ground state to C3-*exo* the transition state; and (d) protonation of N7 of the heterocyclic base. Further work is being carried out on the structure of the enzyme in an attempt to provide information on how the transition state of the 2 deoxyribonucleosides is enforced.

3. Experimental

3.1. Materials

Adenosine nucleosidase was isolated from yellow lupin (*Lupinus luteus*) according to the procedure of Abusamhadneh et al. (2000) to yield an enzyme with a specific activity of 6.3 μmol/min mg (135-fold purification 5.6% yield). [1′-^{13}C], [2′-^{2}H] and [5′-^{2}H]adenosine **1** were obtained from Omicron Biochemicals. [^{15}N]Ammonia (98 at.%) was purchased from Cambridge Isotope Laboratories. 5-Amino-4,6-dichloropyrimidine and [1-^{2}H]ribose were obtained from Aldrich Chemical Co.

3.2. Synthesis of [9-^{15}N]adenine (Sethi et al., 1982)

5-Amino-4,6-dichloropyrimidine (1.75 g; 10.7 mmol) was suspended in 35 mL absolute EtOH in a thick-wall glass reaction tube. The suspension was cooled in an EtOH-dry ice bath and [^{15}N] ammonia (0.7 g; 38.8 mmol) was bubbled through the solution. The reaction tube was sealed and heated to 140 °C in a Parr reaction bomb for 4 h. The reaction mixture was then allowed to cool to room temperature, the solvent was removed under reduced pressure, and the solid was recrystallized from EtOH (yield: 1260 mg; 8.7 mmol; 81%). The product, [4-^{15}N, 5-^{14}N]diamino-6-chloropyrimidine, was authenticated by comparing the melting point, ultraviolet spectrum, and retention time on reverse-phase HPLC to an authentic sample of 4,5-diamino-6-chloropyrimidine. The recrystallized product was dissolved in 10 mL of 1:1 acetic anhydride-triethyl orthoformate and the solution refluxed for 3 h. The reaction mixture was cooled and the solvent removed under reduced pressure. The residue was dissolved in MeOH–H_2O (1:1) and purified by reversed-phase chromatography on an Isco CombiFlash Graduate chromatography system equipped with a Redi-Sep reversed-phase column. The column was eluted with MeOH–H_2O (1:1). Fractions containing [9-^{15}N]6-chloropurine were identified based upon their ultraviolet spectrum and were pooled. The solvent was removed under reduced pressure and dissolved in 15 mL of anhydrous EtOH that was saturated with NH_3. The reaction mixture was sealed in a heavy-wall glass reaction tube and heated to 150 °C for 20 h. After the reaction mixture had cooled, the solvent was evaporated under reduced pressure and the residue recrystallized from EtOH. The product [9-^{15}N]adenine **2** was authenticated by comparing the ultraviolet spectrum and behavior on a C_{18} reversed-phase column (4.6 × 150 mm) eluted with 10 mM ammonium acetate, pH 5.2, 2% methanol with that of an authentic sample of adenine **2**. The extent of isotopic enrichment was determined by mass spectrometry (yield: 558 mg; 4.1 mmol; 38%).

[9-^{15}N]Adenine **2** (250 mg; 1.9 mmol) was suspended in 5 mL anhydrous pyridine and benzoyl chloride (840 mg; 6 mmol) was added. The reaction mixture was refluxed for 2 h and the excess pyridine was removed by distillation. The residue was suspended in saturated $NaHCO_3$ solution and $CHCl_3$ was added. The crude product precipitated, and the crystals were recovered by filtration and washed with H_2O. The product was recrystallized from EtOH to yield N6-benzoyl [9-^{15}N]adenine **2** (354 mg, 1.48 mmol; 78%). The product was authenticated by comparison to a standard sample of N6-benzoyladenine (Bullock et al., 1957).

3.3. Synthesis of 1-O-acetyl 2,3,5-tri-O-benzoyl-β-D-[1-^{2}H]ribofuranoside (Kline and Serianni, 1990)

D-[1-^{2}H]ribose (15.1 g; 100 mmol) was converted to a mixture of methyl α and β [1-^{2}H] ribofuranoside using

the procedure of Barker and Fletcher (1961). [1-^{2}H]ribose was dissolved in 50 mL of anhydrous MeOH with the solvent removed under reduced pressure. This step was repeated two times to remove residual H_2O. The resulting syrup was dissolved in 300 mL anhydrous MeOH and cooled to 4 °C. Concentrated sulfuric acid (1.5 mL) was added and the mixture stirred for 14 h at 4 °C. The reaction mixture was passed through a column of Amberlite IRA-68 resin (40 g resin/mL of acid) in the OH^- form eluted with anhydrous MeOH. The α and β anomers were separated by chromatography on a Dowex 1×2 (200–400) column in the OH^- form eluted with water. Fractions were assayed by phenol-H_2SO_4 test (Chaplin, 1994). The anomers were identified by ^{13}C NMR spectroscopy and those fractions containing the β anomer were concentrated under reduced pressure and crystallized by adding a small seed crystal of methyl β-D-[1-^{2}H]ribofuranoside to the syrup. The crystalline sugar was dried under vacuum at 50 °C (yield: 10.7 g; 6.48 mmol; 65%).

Dried methyl β-D-[1-^{2}H]ribofuranoside (4.9 g; 30 mmol) was dissolved in 20 mL anhydrous pyridine and 25 mL $CHCl_3$. The reaction flask was cooled in an ice bath and 17.5 mL benzoyl chloride (150 mmol) added dropwise with stirring. The reaction mixture was incubated for 12 h at 4 °C and at the end of this time excess benzoyl chloride was decomposed by the addition of 3 g of crushed ice. The reaction mixture was stirred for 2 h at room temperature and the organic phase extracted with 300 mL $CHCl_3$ two times. The $CHCl_3$ layer was dried with anhydrous Na_2SO_4.

The organic phase was evaporated under reduced pressure and dissolved in AcOH (7.5 mL) and Ac_2O (16.9 mL). The solution was cooled, and concentrated H_2SO_4 (2.4 mL) was added slowly. The reaction mixture was stored overnight at 4 °C and the reaction stopped by the addition of 24 g of crushed ice. The reaction mixture was stirred for 30 min and extracted three times with $CHCl_3$ (300 mL). The combined $CHCl_3$ solution was washed with ice-cold saturated $NaHCO_3$ with the organic phase dried (anhydrous Na_2SO_4). The solvent was removed under reduced pressure and product recrystallized from isopropyl alcohol. The product was authenticated by comparison to a standard sample (yield: 11.3 g; 22.5 mmol; 75%).

3.4. Synthesis of labeled ribonucleosides (Kline and Serianni, 1990)

Labeled adenosines were synthesized using a modification of the method of Vorbrüggen (Kline and Serianni, 1990; Vorbrüggen et al., 1981). A reflux apparatus was assembled with 4.1 mmol of the appropriate base (N6-benzoyl adenine or N6-benzoyl [9-^{15}N]adenine) in the reaction flask. After the apparatus was purged with argon, 25 mL hexamethyldisilazane (HMDS) was added followed by 0.5 mL anhydrous pyridine. The suspension was refluxed under argon until the base completely dissolved. Excess HMDS was removed by distillation at atmospheric pressure leaving a clear syrup. The last trace of HMDS was removed by vacuum distillation at 50 °C. The appropriate 1-*O*-acetyl 2,3,5-tri-*O*-benzoyl-β-D-ribofuranoside (2.0 g; 4.0 mmol) was dissolved in anhydrous CH_2Cl_2 (7 mL) and trimethylsilyl trifluoromethanesulfonate added (1.3 mL; 7 mmol). The solution containing the dissolved sugar was added to the reflux apparatus containing the silylated base and the reaction mixture refluxed under argon for 5 h. After the condensation reaction was complete, the reaction mixture was cooled to room temperature and diluted with CH_2Cl_2 (20 mL). The solution was extracted with ice-cold saturated aqueous $NaHCO_3$ solution and the organic phase dried over anhydrous Na_2SO_4. The solvent was removed under reduced pressure at 30 °C. Flash chromatography of the residue on an Isco CombiFlash Graduate chromatography system equipped with a RediSep reversed-phase column was eluted with 90/10 CH_2Cl_2/MeOH. The protecting groups were removed by dissolving the sample in MeOH saturated with ammonia and incubating at 25 °C for 24 h. The solvent was removed under reduced pressure at 30 °C and the residue dissolved in distilled H_2O. The aqueous solution was extracted three times with $CHCl_3$ and Et_2O. The H_2O was removed under reduced pressure with the resulting syrup chromatographed on a Dowex 1×2 column in the OH^- form eluted with H_2O–MeOH (7:3) followed by H_2O–MeOH (2:3). Labeled adenosine-containing fractions were pooled and concentrated to yield 643 mg, 2.4 mmol, 60%. The identity of the product was confirmed by ^{1}H NMR spectroscopic analysis and the extent of isotopic enrichment a determined by LC/MS.

3.5. Measurement of kinetic isotope effects

Heavy atom kinetic isotope effects were measured using a modification of the competitive method developed for stable isotopes (Parkin, 1991; Hunt et al., 2005). A reaction mixture consisting of 50% specifically labeled and 50% unlabeled adenosine **1** (1 mM total concentration) in 10 mM Tris, pH 7.2, was divided into two portions. The reaction was initiated by the addition of adenosine nucleosidase and incubated at 37 °C. The progress of the reaction was monitored by reversed-phase HPLC on a ODS column eluted with 95%, 10 mM ammonium acetate, pH 5.2; 5% methanol. One reaction mixture was allowed to continue to between 20% and 30% completion and the other allowed to continue to 100% completion as determined by HPLC. The reactions were stopped by the addition of 100 μL of 1 M HCl.

The isotopic composition of the appropriate product, either ribose or adenine, depending on the location of the label, was determined by chromatography on a Hewlett Packard liquid chromatograph interfaced to an atmospheric pressure interface-electrospray mass spectrometer (LC/MS). A sample volume of 5 μL was injected onto a Hypersil ODS column (100×2.1 mm) using water as the mobile phase. The mass spectrometer was operated in the

positive ion mode with a gas temperature of 350 °C, drying gas flow rate of 13.0 L/min, a nebulizer pressure of 25 psig, and a fragmentor voltage of 40. Mass spectra for labels in the ribose moiety were collected at 173 and 174 amu under selected ion monitoring (SIM) conditions. For labels in the adenine **2** moiety, mass spectra were collected at 158 and 159 amu under SIM conditions. The isotopic composition was determined by extracting the appropriate ions from the mass chromatogram and integrating the resulting peaks.

The kinetic isotope effects were calculated by measurement of the relative rates of hydrolysis of the nucleoside containing a light (natural abundance) or heavy atom in a given position. As measurement of kinetic isotope effects using stable isotopes uses concentrations of labeled substrate comparable to that of unlabeled substrate, the equations used to calculate the kinetic isotope effects must be modified from those used for radio-labeled substrates (Berti et al., 1997). The kinetic isotope effects were calculated using the following formula:

$$\text{kinetic isotope effect} = \frac{\ln[(1-f)(1+r_0^{-1})/(1+r_i^{-1})]}{\ln[(1-f)(1+r_0)/(1+r_i)]}, \quad (2)$$

where f is the fraction of substrate hydrolyzed as determined by HPLC and r_i and r_0 are the ratio of peak intensities, after correction for natural abundance, of unlabeled/labeled products at the times the reaction was stopped and started, respectively. The family of kinetic isotope effects was used to determine the transition state as described below.

3.6. Transition-state modeling

An ad hoc bond-energy bond-order vibrational analysis was used to match experimental intrinsic kinetic isotope effects for [9-^{15}N], [1′-^{13}C], [1′-^{2}H], [2′-^{2}H], and [5′-^{2}H]adenosine **1** to proposed transition states using the BEBOVIB-IV program from the Quantum Chemistry Program Exchange (Sims et al., 1977; Berti and Tanake, 2002). Due to the limitation on the maximum number of atoms available in the BEBOVIB-IV program, a cutoff model containing only relevant atoms was used (Sims and Lewis, 1984). The atoms omitted in the construction of the cutoff model for transition state modeling were the 2, and 5 hydroxylic hydrogen atoms and the 3 hydroxyl group of the ribose ring along with N1, C2, and the exocylic amino group of the purine ring. Force constants for the various vibrational modes were derived from reported values (Sims et al., 1977; Sims and Lewis, 1984). The starting point for the ground-state of adenosine was its crystal structure (Lai and Marsh, 1972). This structure was then energy minimized using Spartan 5 and Gaussian 98w (Fig. 1). Transition-state structures were varied systematically to match the observed kinetic isotope effects. The acceptable transition state gave a chemically reasonable structure that matched the intrinsic kinetic isotope effects.

Acknowledgement

This work was supported by an American Chemical Society Petroleum Research Fund Type B Grant (# 33688-B4).

References

Abusamhadneh, E., McDonald, N., Kline, P.C., 2000. Isolation and characterization of adenosine nucleosidase from yellow lupin (*Lupinus luteus*). Plant Sci. 153, 25–32.

Barker, R., Fletcher Jr., H.G., 1961. 2,3,5-Tri-*O*-benzyl-D-ribosyl and -L-arabinosyl bromides. J. Org. Chem. 26, 4605–4609.

Berti, P., Blanke, S.R., Schramm, V.L., 1997. Transition state structure for the hydrolysis of NAD^+ catalyzed by diphtheria toxin. J. Am. Chem. Soc. 119, 12079–12088.

Berti, P.J., Schramm, V.L., 1997. Transition state structure of the solvolytic hydrolysis of NAD^+. J. Am. Chem. Soc. 119, 12069–12078.

Berti, P.J., Tanake, K., 2002. Transition state analysis using multiple kinetic isotope effects: mechanisms of enzymatic and non-enzymatic glycoside hydrolysis and transfer. In: Tidwell, T.T., Richard, J.P. (Eds.), Advances in Physical Organic Chemistry, vol. 37. Academic Press, San Diego, pp. 239–314.

Bullock, M.W., Hand, J., Stokstad, E., 1957. Reduction of 6-aroylaminopurines with lithium aluminum hydride. J. Org. Chem. 22, 568–569.

Burch, L.R., Stuchbury, T., 1986. Purification and properties of adenosine nucleosidases from tomato (*Lycopersicon esculentum*) roots and leaves. J. Plant Physiol. 125, 267–273.

Campos, A., Rijo-Johansen, M., Carneiro, M., Fevereiro, P., 2005. Purification and characterization of adenosine nucleosidase from *Coffea arabica* young leaves. Phytochemistry 66, 147–151.

Chaplin, M.F., 1994. Monosaccharides. In: Chaplin, M.F., Kennedy, J.F. (Eds.), Carbohydrate Analysis: A Practical Approach. IRL Press, New York, pp. 2–3.

Chen, C.M., Kristopeit, S.M., 1981. Metabolism of cytokinin: deribosylation of cytokinin ribonucleosides by adenosine nucleosidase from wheat germ. Plant Physiol. 68, 1020–1023.

Chen, X-Y., Berti, P.J., Schramm, V.L., 2000. Transition-state analysis for depurination of DNA by ricin-A chain. J. Am. Chem. Soc. 122, 6527–6534.

Degano, M., Almo, S., Sacchettini, J.C., Schramm, V.L., 1998. Trypanosomal nucleoside hydrolase. A novel mechanism from the structure with a transition-state inhibitor. Biochemistry 18, 6277–6285.

Degano, M., Gopaul, D., Scapin, G., Schramm, V.L., Sacchetini, J., 1996. Three-dimensional structure of the inosine–uridine nucleoside *N*-ribohydrolase from *Crithidia fasciculata*. Biochemistry 35 (1996), 5971–5981.

Edwards, R., 1996. *S*-adenosyl-L-methionine metabolism in alfalfa cell cultures following treatment with fungal elicitors. Phytochemistry 43, 1163–1169.

Estupiñán, B., Schramm, V.L., 1994. Guanosine–inosine-preferring nucleoside *N*-glycohydrolase from *Crithidia fasciculata*. J. Biol. Chem. 37, 23066–23073.

Garrett, E.R., Mehta, P.J., 1972. Solvolysis of adenine nucleosides. I. Effects of sugar and adenine substituents on acid solvolysis. J. Am. Chem. Soc. 94, 8532–8541.

Gopaul, D., Meyer, S., Degano, M., Sacchettini, J., Schramm, V.L., 1996. Inosine–uridine nucleoside hydrolase from *Crithidia fasciculata*. Genetic characterization, crystallization, and identification of histidine 241 as a catalytic site residue. Biochemistry 35, 5963–5970.

Guranowski, A., Schneider, Z., 1977. Purification and characterization of adenosine nucleosidase from barley leaves. Biochim. Biophys. Acta 482, 145–158.

Guthrie, R.D., Jencks, W.P., 1989. IUPAC recommendations for the representation of reaction mechanisms. Acc. Chem. Res. 22, 343–349.

Horenstein, B.A., Parkin, D.W., Estupiñán, B., Schramm, V.L., 1991. Transition-state analysis of nucleoside hydrolase from *Crithidia fasciculata*. Biochemistry 30, 10788–10795.

Horenstein, B.A., Zabinski, R.F., Schramm, V.L., 1993. A new class of C-nucleoside analogues-1-(*S*)-aryl-1,4-dideoxy-1,4-imino-D-ribitols, transition state analogue inhibitors of nucleoside hydrolase. Tetrahedron Lett. 34, 7213–7216.

Hunt, C., Gillani, N., Farone, A., Rezaei, M., Kline, P., 2005. Kinetic isotope effects of nucleoside hydrolase from *Escherichia coli*. Biochim. Biophys. Acta 1751, 140–149.

Imagawa, H., Yamano, H., Inoue, K., Takino, Y., 1979. Purification and properties of adenosine nucleosidases from tea leaves. Agric. Biol. Chem. 43, 2337–2342.

Kline, P.C., Serianni, A., 1990. ^{13}C-enriched ribonucleosides: Synthesis and application ^{13}C–^{1}H and ^{13}C–^{13}C spin-coupling constants to assess furanose and *N*-glycoside conformations. J. Am. Chem. Soc. 112, 7373–7381.

Koerner, T., Westaway, K.C., Poirier, R.A., Wang, Y., 2000. An unusually large secondary α-deuterium kinetic isotope effect in hydride ion S_N2 reactions. Can. J. Chem. 78, 1067–1072.

Koshiishi, C., Kato, A., Yama, S., Crozier, A., Ashihara, H., 2001. A new caffeine biosynthetic pathway in tea leaves: utilization of adenosine released from the *S*-adenosyl-L-methionine cycle. FEBS Lett. 499, 50–54.

Kurtz, J., Exinger, F., Erbs, P., Jund, R., 2002. The *URH1* uridine ribohydrolase of *Saccharomyces cerevisiae*. Curr. Genet. 41, 132–141.

Lai, T.F., Marsh, R.E., 1972. The crystal structure of adenosine. Acta Crystallogr., Sect. B 28, 1982–1989.

Lee, W.J., Pyler, R.E., 1986. Nucleic acid degrading enzymes of barley mait. III. Adenosine nucleosidase from malted barley. Am. Soc. Brew. Chem. J. 44, 86–90.

Le Floc'h, F., Lafleuriel, J., 1981. The purine nucleosidases of Jerusalem artichoke shoots. Phytochemistry 20, 2127–2129.

Leszczynska, D., Schneider, Z., Tomaszewski, M., Mackowiak, M., 1984. Comparative studies on adenosine nucleosidase occurrence in plants. Ann. Botany 54, 847–849.

Matsson, O., Westaway, K.C., 1998. Secondary deuterium kinetic isotope effects and transition state structure. In: Bethell, D. (Ed.), Advances in Physical Organic Chemistry, vol. 31. Academic Press, San Diego, pp. 143–248.

Mazzella, L.J., Parkin, D.W., Tyler, P., Furneaux, R., Schramm, V.L., 1996. Mechanistic diagnoses of *N*-ribohydrolases and purine nucleoside phosphorylase. J. Am. Chem. Soc. 118, 2111–2112.

Melander, L., Saunders Jr., W.H., 1980. Reactions Rates of Isotopic Molecules. Wiley, New York, pp. 74–75.

Mentch, F., Parkin, D.W., Schramm, V.L., 1987. Transition-state structure for *N*-glycoside hydrolysis of AMP by acid and by AMP nucleosidase in the presence and absence of allosteric activator. Biochemistry 26, 921–930.

Miller, R.L., Sabouring, C., Krenitsky, T., Berens, R., Marr, J., 1984. Nucleoside hydrolases from *Trypanosoma cruzi*. J. Biol. Chem. 259, 5073–5077.

Murzin, A.G., Brenner, S.E., Hubbard, T., Chothia, C., 1995. SCOP: A structural classification of proteins database for the investigation of sequences and structures. J. Mol. Biol. 247, 536–540.

Orengo, C.A., Michie, A.D., Jones, S., Jones, D.T., Swindells, M.B., Thornton, J.M., 1997. CATH – a hierarchic classification of protein domain structures. Structure 5, 1093–1108.

Parkin, D.W., 1991. Methods for the determination of competitive and noncompetitive kinetic isotope effects. In: Cook, P.F. (Ed.), Enzyme Mechanism from Isotope Effects. CRC Press, Boca Raton, FL, pp. 269–290.

Parkin, D.W., 1996. Purine-specific nucleoside *N*-ribohydrolase from *Trypanosoma brucei brucei*. Purification, specificity, and kinetic mechanism. J. Biol. Chem. 271, 21713–21719.

Parkin, D.W., Horenstein, B., Abdulah, D.R., Estupiñán, B., Schramm, V.L., 1991a. Nucleoside hydrolase from *Crithidia fasciculata*. Metabolic role, purification, specificity, and kinetic mechanism. J. Biol. Chem. 266, 20658–20665.

Parkin, D.W., Mentch, F., Banks, G., Horenstein, B., Schramm, V.L., 1991b. Transition-state analysis of a V_{max} mutant AMP nucleosidase by the application of heavy-atom kinetic isotope effects. Biochemistry 30, 4586–4594.

Pelle, R., Schramm, V.L., Parkin, D.W., 1998. Molecular cloning and expression of a purine-specific *N*-ribohydrolase from *Trypanosoma brucei brucei*. Sequence, expression, and molecular analysis. J. Biol. Chem. 273, 2118–2126.

Petersen, C., Moller, L.B., 2001. The *rihA*, *rihB*, and *rihC* ribonucleoside hydrolases of *Escherichia coli*. J. Biol. Chem. 276, 884–894.

Poirier, R.A., Wang, Y., Westaway, K.C., 1994. A theoretical study of the relationship between secondary α-deuterium kinetic isotope effects and the structure of S_N2 transition states. J. Am. Chem. Soc. 116, 2526–2533.

Poulton, J.E., Butt, V.S., 1976. Partial purification and properties of adenosine nucleosidase from leaves of spinach beet (*Beta vulgaris* L.). Planta 131, 179–185.

Schramm, V.L., Horenstein, B.A., Kline, P.C., 1994. Transition state analysis and inhibitor design for enzymatic reactions. J. Biol. Chem. 269, 18259–18262.

Sethi, S., Gupta, S., Jenkins, E., Townsend, L., McCloskey, J., 1982. Mass spectrometry of nucleic acid constituents. Electron ionization spectra of selectively labeled adenines. J. Am. Chem. Soc. 104, 3349–3353.

Shi, W., Schramm, V.L., Almo, S., 1999. Nucleoside hydrolase from *Leishmania major*. Cloning, expression, catalytic properties, transition state inhibitors, and the 2.5 Å crystal structure. J. Biol. Chem. 274, 21114–21120.

Sims, L.B., Burton, G.W., Lewis, D.E., 1977Quantum Chemistry Program Exchange, vol. 337. Indiana University, Bloomington, IN.

Sims, L.B., Lewis, D.E., 1984. Bond order methods for calculating isotope effects in organic reactions. In: Buncel, E., Lee, C.C. (Eds.), Isotopes in Organic Chemistry, vol. 6. Elsevier Science, New York, pp. 161–259.

Stern, M.J., Wolfsberg, M., 1966. Simplified procedure for the theoretical calculation of isotope effects involving large molecules. J. Chem. Phys. 45, 4105–5124.

Swain, C.G., Stivers, E.C., Reuwer, J.F., Schaad, L.J., 1958. Use of hydrogen isotope effects to identify the attacking nucleophile in the enolization of ketones catalyzed by acetic acid. J. Am. Chem. Soc. 80, 5885–5893.

Versées, W., Decanniere, K., Pelle, R., Depoorter, J., Brosens, E., Parkin, D.W., Steyaert, J., 2001. Structure and function of a novel purine specific nucleoside hydrolase from *Trypanosoma vivax*. J. Mol. Biol. 307, 1363–1379.

Versées, W., Decanniere, K., Van Holsbeke, E., Devroede, N., Steyaert, J., 2002. Enzyme-substrate interactions in the purine-specific nucleoside hydrolase from *Trypanosoma vivax*. J. Biol. Chem. 277, 15938–15946.

Versées, W., Steyeart, J., 2003. Catalysis by nucleoside hydrolases. Curr. Opin. Struct. Biol. 13, 731–738.

Vorbrüggen, H., Krolikiewicz, K., Bennua, B., 1981. Nucleoside synthesis with trimethylsilyl triflate and perchlorate as catalysts. Chem. Ber. 114, 1234–1255.